[Article] SOFT TISSUE DIAGNOSIS IN MAXILLOFACIAL SURGERY: A PRELIMINARY STUDY ON THREE-DIMENSIONAL FACE GEOMETRICAL FEATURES BASED ANALYSIS

SOFT TISSUE DIAGNOSIS IN MAXILLOFACIAL SURGERY: A PRELIMINARY STUDY ON THREE-DIMENSIONAL FACE GEOMETRICAL FEATURES BASED ANALYSIS

F. Calignano, E. Vezzetti

Dipartimento di Sistemi di Produzione Ed Economia dell'Azienda, Politecnico di Torino, Corso Duca degli Abruzzi 24, 10129,Torino, Italy

Tel.: +39 011 5647294; Fax: +39 011 5647299; e-mail: enrico.vezzetti@polito.it

Abstract

To obtain the best surgical results in orthognathic surgery, treatment planning and the evaluation of results should be performed. In these operations it is necessary to provide to the physicians powerful tools able to underline the behaviour of soft tissue. For this reason, considering the improvements provided by the use of 3D scanners in the medical diagnosis this paper proposes a methodology for analysing the facial morphology working with geometrical features. The methodology has been tested over patients affected by malocclusion, in order to analyse the reliability and efficiency of the provided diagnostic results.

Keywords: 3DScanner, Shape analysis, Facial Morphology, Soft-tissues Shifts

Introduction

The assessment of the dimensions and arrangement of facial soft tissues is important for medical evaluations. Orthodontists, orthognathic maxillofacial and plastic surgeons often require quantitative data about the correlation between soft and hard tissues[1,2]. For many years these information have been obtained from 2D radiographies and photos, even if these have been consistently limited [3,4,5,6]. Significant improvements have been obtained with the use of computer vision algorithms even if the use of bi-dimensional supports to analyze three-dimensional objects seems to be quite inadequate. For this reason, many research efforts of the last ten years have been directed to develop computer vision tools, that with the use of 3D scanner devices are able to provide reliable and more complete data. These systems use different technologies, like active or passive light reflection analysis and are able to describe 3D real shapes with a point cloud, analyzable with 3D software. But while the image processing methodologies are well known in the medical context, the situation for 3D scanners is still quite marginal and fragmented.

Some studies have been developed for proposing structured procedures that could be used for driving physicians in the application of 3D scanner to medical diagnosis [7,8,9,10,12], but anyway at present no one succeeded in the development of a standardized strategy and accepted by the whole medical context.

Actually it is possible to move from morphometric tools that implement statistical shape analysis as Generalised Procrustes Superimposition (GPS) and Principal Component Analysis (PCA). The first iterative method (GPS) applies geometrical transformations (scales, traslations, rotations and reflections) in order to compare reference points (landmarks) [13,14] taken from different point clouds of the patient's face. The PCA method evaluates the tendency of the landmarks distribution along x and y axis, locating a new working frame, centred on the average shape centre. The method creates new variables named principal components (PCs), that describe how much the landmark configuration of each sample is different from the average shape. Moving to the 2D radiographies the Thin-Plate Spline analysis (TPS) allows to work on a point set of anatomical landmarks over the pre and post surgery radiography. Then the post-surgery radiography is considered as an infinitely thin metal plate that must be bended, in a direction orthogonal to the plane, in order to match its landmarks to the pre-surgery radiography, while the bending energy it's minimized[15,16,17]. If the two shapes are identical, the bending energy is zero and the plate is flat. In order to provide information regarding the face morphology also in the regions around landmarks, the Multi Sectional Spline method employs section planes passing through a set of specific reference points of a point cloud (landmarks), in order to obtain a specific section spline. The shifts of the facial morphology between the pre and post surgery point clouds can be analyzed by comparing the two section profiles passing through homologous landmarks and section planes[18,19]. Working with the entire points cloud, instead of some portions only, with the Clearance Vector Mapping method (CVM), the pre and post surgery point clouds are firstly aligned (ICP, CSM, . . .) [20,21] and then the magnitude of the 3D shape displacement can be computed working on triangulated meshes, following different approaches (radial, normal, …) [22], showing the displacement with a colour mapping. At present even if the most employed methodology for the maxillo-facial diagnosis still remains the conventional cephalometric analysis (CCA) [11], the Multisectional Splines seems to be the most reliable and complete methodology, because it is able to provide reliable information

about the tissues shifts, as the CCA approach, but is also able to provide additional global information, as for instance some pathologies as lateral asymmetry.

Anyway there are some significant points on which it is necessary in order to work to develop a diagnostic procedure that could be accepted by the entire medical context. It is necessary to define a method that extracts shape morphology measures, starting from the landmarks as reference points, so to guarantee consistent morphological comparison, but also considering the entire facial shape (point cloud) so to consider each useful information.

For this reason at present some studies [23,24,25,26] have tried to exploit the three-dimensional information coming from non invasive 3D scanner as laser scanners extracting area and volume measures. One of the most significant study [27] has worked on soft tissues landmarks creating a geometrical model approximating the face features with flat triangles which vertexes have been represented by the facial landmarks.

This approach has provided a simple and direct methodology for supporting the evaluation of facial areas and volumes. But while the morphological behaviour of the face is characterised by smooth surfaces, this methodology working with flat triangles is only able to provide a first approximation of the face behaviour neglecting a series of features. Considering that 3D scanners provide accurate points cloud it would be more useful to employ methodologies able to exploit the entire point cloud morphology.

So starting from this concept the idea of the proposed methodology would maintain the concept employing geometrical features for approximating the facial shape, but instead of using only tetrahedron for describing the face morphology, proposes to employ different three-dimensional geometries able to fit better the face morphology.

The proposed methodology: Geometrical Features Based Approach

In order to identify the geometries to employ for developing a geometrical features based model, it has been necessary to define how to decompose the facial morphology. Starting from the head modelling guide lines [28] and from the facial soft tissue landmarks coordinates (Tab.1), the face has been divided in four different regions (Fig.1), sectioning the model with a series of planes passing throw: *vertex, upper and lower part of the nose and throw the chin.*

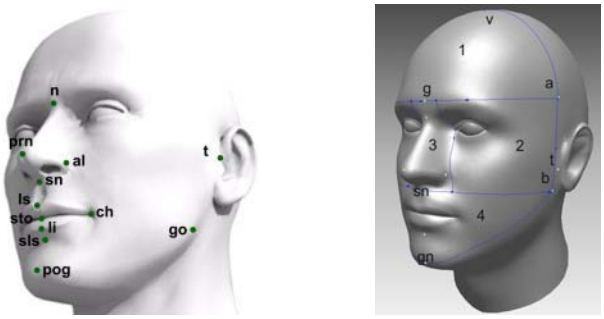

Figure 1: Soft-tissue Landmarks and face decomposition

Soft tissue landmarks	
Name	**Abbr.**
Nasion	n
Pronasale	prn
Subnasale	sn
Labiale superius	ls
Stomion	sto
Labiale inferius	li
Sublabiale	sls
Pogonion	pog
Tragion	t_{right}, t_{left}
Nasal alar crest	al_{right}, al_{left}
Cheilion	ch_{right}, ch_{left}
Gonion	go_{right}, go_{left}
Vertex	v

Table 1: List of soft tissue morphological reference points (landmarks)

Once defined the four regions, for every zone it has been necessary to evaluate which geometry would be more suitable for fitting the different possible shapes that the region could show. Starting from the number of landmarks, characterising every identified region, from the available three-dimensional geometries and from the all different possible facial morphologies, working with some hypothesis developed on the correlations between the cranial shapes and polygons [29,30,31], it has been possible to identify the best fitting geometries [32]:

- **Zone 1:** (*upper face portion*) this region could be described by an ellipsoid with the following parametric formula:

$$\begin{aligned} x &= a\cos\theta\sin\varphi \\ y &= b\sin\theta\sin\varphi \\ z &= c\cos\varphi \end{aligned} \qquad (1)$$

where $\theta \in [0,2\pi]$ and $\varphi \in [0,\pi]$ and *a, b, c* are the semi axis lengths. More precisely it is necessary only an ellipsoid quarter which axis 2*a*, 2*b* and 2*c* are correlated with the landmarks. The first axis *2a* represents the head thickness *(eu-eu)*. The second axis *2b* is the head horizontal length *(g-a)*, evaluated from the glabella *(g)* till the point located on the orthogonal plane *(a)* passing throw the tragion *(t)*. The last axis *2c* is represented by the frontal height (Fig.2).

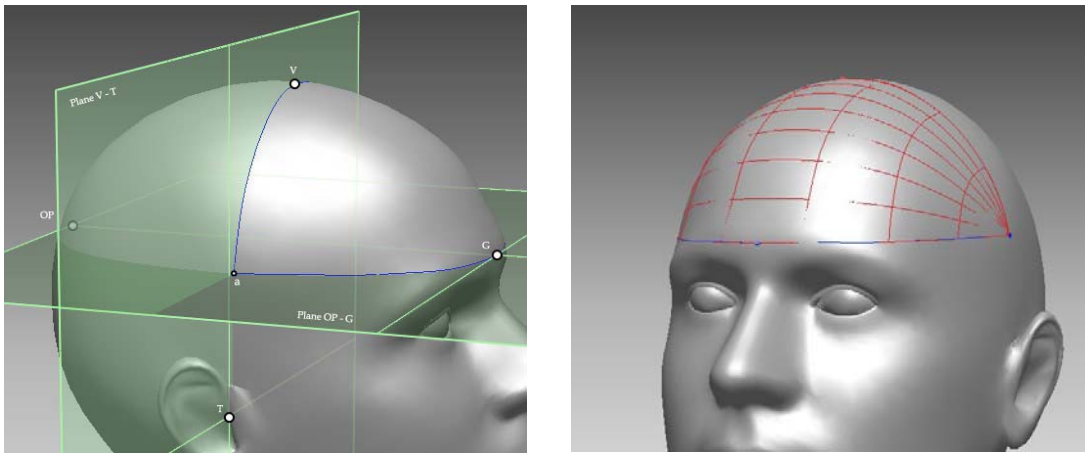

a) **b)**

Figure 2: Upper face portion geometrical feature: a) landmarks b) ellipsoid

- **Zone 2**: (*middle face portion*) this region could be described by a cylinder with elliptical shape with the following parametric formula:

$$\begin{aligned} x &= a\cos u \\ y &= b\sin u \\ z &= v \end{aligned} \qquad (2)$$

where $u \in [0,2\pi]$ and $v \in [0,h]$ and *a* is the semi major axis, *b* the semi minor axis and *h* its eight. This region should be constrained by the following references: the plane passing throw *g-op*, the plane parallel to *g-op* and passing throw *sn*, the plane passing throw *v-t* and the plane parallel to plan *v-t* and passing throw the ear lobe attachment point (Fig.3)

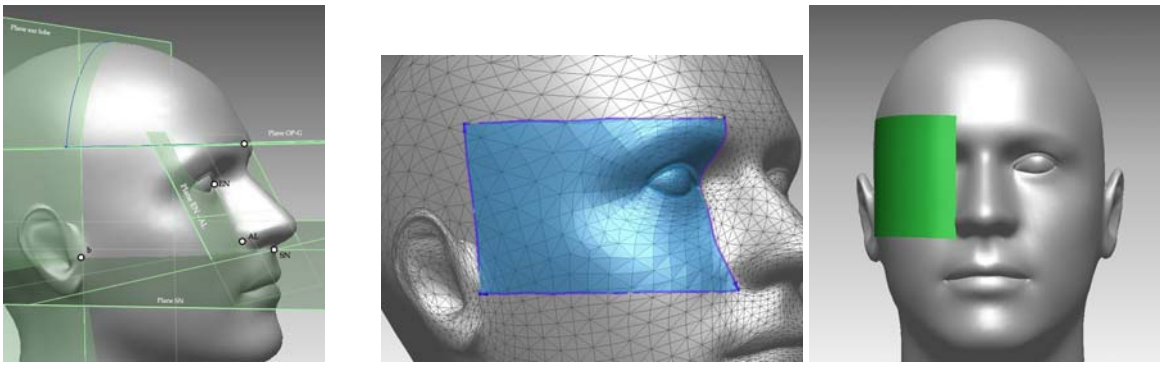

a) b) c)

Figure 3: Middle face portion geometrical feature: a) landmarks b) evidenced area c) cylinder

- **Zone 3**: (*nose*) : the nose could be described by a conical frustum with elliptical base which parametric formula could be obtained from the elliptical cone one:

$$\begin{aligned} x &= a\frac{h-u}{h}\cos\theta \\ y &= b\frac{h-u}{h}r\sin\theta \\ z &= u \end{aligned} \qquad (3)$$

where $u \in [0,h]$ and $\theta \in [0,2\pi]$ while *h is* the eight. The geometry could be built passing throw the following fundamental landmarks: nasion *(n)*, endocanthion *(en_{sx},en_{dx})*, pronasale *(prn)*, subnasale *(sn)*, and left nasal alae and right nasal alae *(al_{sx}, al_{dx})* (Fig.4).

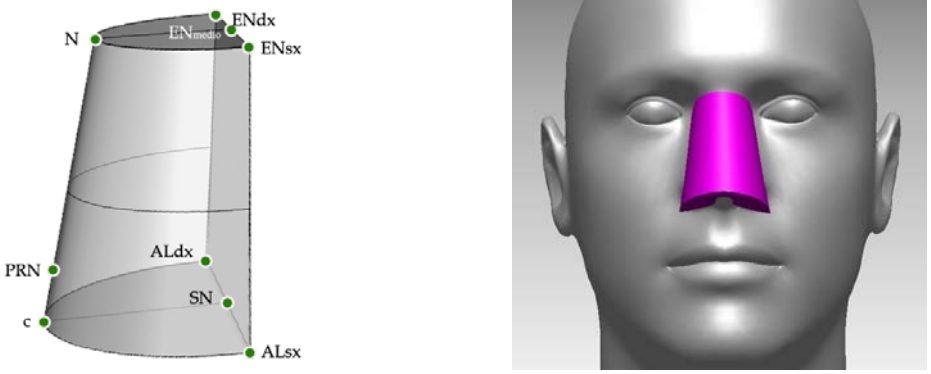

a) **b)**

Figure 4: Lower face portion geometrical feature: a) landmarks b) conical frustum

- **Zone 4**: (*lower face portion*) this region could be described by an ellipsoid with the following parametric formula:

$$\begin{aligned} x &= a\cos\theta\sin\varphi \\ y &= b\sin\theta\sin\varphi \\ z &= c\cos\varphi \end{aligned} \qquad (4)$$

where $\theta \in [0,2\pi]$ and $\varphi \in [0,\pi]$ and *a, b, c* are the semi axis lengths. The quarter of ellipsoid (Fig.5) would be characterised by the first axis *a* that is represented by the bi-zygomatic *(zi_{sx}-zi_{dx})* and the bigonial *(go_{sx}-go_{dx})* largeness. The second axis *b* is obtained as the horizontal length *sn-b* evaluated on the subnasale *(sn)* point till

the point *(b)* located on an orthogonal plane passing throw the tragion *(t)*. The last axis *c* is represented by the distance between the subnasale *(sn)* and the gnathion *(gn)*.

a) b)

Figure 5: Lower face portion geometrical feature: a) landmarks b) ellipsoid

Methodology Validation

In order to evaluate the performances of the proposed methodology, two experimental approaches have been implemented working on a specific facial malformation and analysing five patients. In the first experimental phase the proposed methodology has been compared with the morphological data obtained with the use the traditional Cephalometric method (CCA). In the second phase the proposed methodology has been employed in order to evaluate the soft-tissue areas before and after the surgery and these results have been compared with those obtained with the tetrahedron methodology [1].

Case Studies: Pathology and Tools

The selection of the facial pathology has been driven by the necessity of a simple surgery treatment to allow a simple understanding of the correlation between hard tissue modifications and soft tissue shifts. The selected facial pathology is the "malocclusion" characterized by the misalignment between upper and lower mandibular structures (Fig.6), that is treated with a surgical traslation of the mandible.

a) b) c)

Figure 6: Schematic example of malocclusion: a) Class I, b) Class II, c) Class III

All the patients employed for the case studies are Caucasian, around thirty-five years old, and treated with bilateral sagittal split osteotomy surgery (BSSO) [33]. The case studies (Fig.7) have been selected first of all in relation to the availability of the persons to be involved in this experimentation, but also because of the entity of their pathology. In fact while both the first, the second, the fourth and fifth patients were affected by malocclusion class two, the intensity of these malformations were different. Both in the fourth and fifth patients the malocclusion show a strong redicing effect, in the other two, showing at the same a significant mastication problem, the pathology is less evident. This choice has been driven by the necessity to verify the behavior of the proposed methodology in relation to the entity of the correction to be implemented. In order to provide a more complete experimental validation also a class three malocclusion has been selected, with the introduction of the patient three in the case studies set.

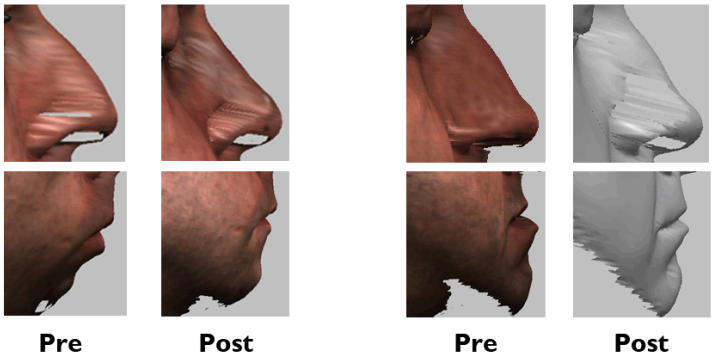

Figure 7: case studies employed – Malocclusion Class II and Malocclusion Class III

The method has been implemented over the five patients, pre and post surgery, acquired with the use of a 3D laser scanner *Cyberware Scanner 3030RGB* (Cyberware Laboratories, Inc., Monterey, California) specific for human head acquisition (Fig. 8).

Figure 8: The 3D Scanner Cyberware 3030RGB

Case Studies: CCA Evaluation vs Geometrical features based analysis

In order to provide a consistent validation of the proposed methodology first of all the five patients have been analysed with the consolidated conventional chephalometric method (CCA)

One measures family of significant anthropometric points (landmarks) has been evaluated over the facial shape to perform a reliable and consistent comparison of the methods. The measures have been evaluated over the hard (skeletal) tissues, employing radiographies.

Hard tissue landmarks	
Name	**Abbr.**
Nasion	N
Menton	ME
Anterior nasal spine	SNA
Gnathion	GN
Articulare	AR
Gonion	GO

Table 2: List of hard tissue morphological reference points (landmarks)

Although the geometrical features based method employs the soft-tissues landmarks, while the CCA uses the second one, the comparison between the two methods, will be at the same possible and reliable, because soft tissue reference points overlap the hard tissue reference points, with a known shift given by the average thickness of the facial soft tissue.

Over the identified hard-tissue some cephalometric angular and linear measurements have been defined (Fig.9). The linear measures are: *the facial height of the anterior face (N-ME), the anterior upper height of the face (N-SNA), the anterior lower height of the face (SNA-ME), the posterior height of the face (S-GO), the upper posterior height of*

the face (S-AR), the lower posterior height of the face (AR-GO). The angular measurements are: *(ARGO-GOGN) who describe the slope of the mandibular plane relative to the anterior base of the skull as angle between the (AR-GO) line and the mandibular plane (GO-GO) and the Gnathion angle (ARGO-GOME) who describes the slope of the ramous relative to the mandible body as angle between the (AR-GO) line and (GO-ME) line*.

Looking at the results obtained over the five patients (Tab. 3) it is possible to see that after the surgery the lower part of the facial profile *(SNA-ME)* has increased its length, with a consequent reduction of the upper part of the face *(N-SNA)*. This is also confirmed by the *Index of Anterior Facial Ratio (IPFA)*, namely the ratio between *(N-SNA)* and *(SNA-ME)*, that decreases its value of 0.85 in the pre-surgery face profile, to the value of 0,75 in the post surgery. Following the medical standards proportions *(N-SNA)* represents the 45% of the total facial length and *(SNA-ME)* is the 55%. In the case studies analysed in the pre-surgery morphology the proportions are maintained, but not in the post surgery, where the evaluated differences from the standard percentage are around 3%.

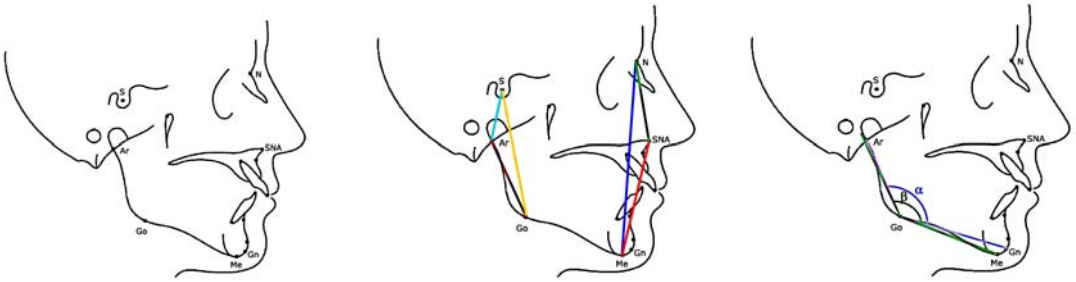

a) b) c)

Figure 9: a) Graphical location of soft tissue landmarks, b-c) Three-Dimensional Chephalometric Measures

In order to verify the mandibular modification with the other measures, the goniac angle β has been measured. Moving from pre to post-surgery facial shape, this value has shown a significant increasing probably due to the rise of the measure *(Ar-Go)*. To verify this hypothesis, the goniac angle β has been divided in two parts: the lower and upper goniac angle, that have been separately evaluated. The ratio between standard deviation σ and average value μ, of the two portions of the goniac angles also show that the lower goniac angle has a more stable behaviour, so it could give more reliable information about the facial shift between pre and post-surgery (Tab.4)

Measure	Pre-surgery					Post-surgery					Significance analysis		
	Face 1	Face 2	Face 3	Face 4	Face 5	Face 1	Face 2	Face 3	Face 4	Face 5	μ	σ	σ/μ
Lower Face													
ArGo-GoGn (α)	130.02	134.76	148.52	136.51	131.3	134.67	134.36	152.19	136.19	129.8	1.22	2.74	2.25
ArGo-GoMe (β)	136.26	139.1	151.37	138.65	132.49	139.81	140	156.6	139.16	136.08	2.75	1.99	0.72
S-Go	68.88	75.77	71.95	62.66	62.01	90.17	71.29	57.48	61.02	64.25	0.58	13.12	22.32
N-Me	126.68	111.95	135.35	117.36	116.36	125.22	110.8	126.41	116.58	124.53	0.83	6.07	7.29
SNA-Me	70.44	64.29	88.04	72.33	67.93	82.46	64.96	87.08	72.76	77.43	4.33	5.97	1.38
Ar-Go	65.37	57.95	55.14	59.4	48.57	67.93	58.03	44.68	59.5	51.99	0.86	5.57	6.47
Middle Face													
S-Ar	16.6	16.55	22.95	17.25	17.31	18.48	13.58	16.12	15.82	14.6	2.41	3.14	1.3
N-SNA	68.53	64.68	64.21	57.85	54.47	52.72	58.86	59.54	58.29	58.28	4.44	7.48	1.68

Table 3: Angular and linear cephalometric measures with the significance analysis of the pre and post-surgery facial morphology modifications (Average **μ,** Standard Deviation **σ**) [mm]

In the pre and post-surgery, both angles (Fig.10) are different from the standard values: the upper goniac angle is bigger than 55° and the lower goniac angle is smaller than 70°, but the surgery treatment has caused an horizontal increasing of the mandible measures, bringing them towards more normal values. Moreover considering that only *Go* and *Me* could move in relation with the surgery, while *N* and *Ar* are fixed, it is possible to justify while malocclusion class II patients have been characterized by an increased lower goniac angle, while the class III one shows a reduction.

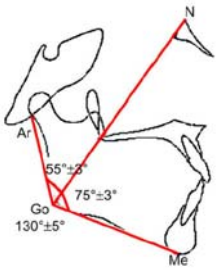

Figure 10: Lower and upper goniac angles with standard values

Measure	Pre-surgery					Post-surgery					Significance analysis		
	Face 1	Face 2	Face 3	Face 4	Face 5	Face 1	Face 2	Face 3	Face 4	Face 5	μ	σ	σ/μ
$Ar\hat{G}oN$	72.57	77.37	77.09	73.72	64.29	72.34	71.81	80.69	71.91	69.38	0.22	4.27	19.58
$N\hat{G}oMe$	66.98	62.29	74.50	64.10	72.48	63.95	65.66	74.15	62.80	68.85	1.07	2.61	2.45

Table 4: Measures of Lower and Upper goniac angles [deg]

From this analysis it is possible to see that the most significant shifts have been verified on the nose and the lower face portion.

Working with geometrical features based method the results confirm that the most significant shifts have been verified over the lower facial portion and over the middle facial portion with the most significant shifts evidenced over the nose. From a first global visual analysis implemented over the different geometrical features before and after the surgery, it is possible to see an increasing of the length of the lower face portion, together with a middle face portion reduction.

For obtaining a more complete description of the soft tissues shifts all over the face, in particular how the lower face surgery could influence also the upper area, also the nose has been evaluated. For this purpose, some morphological measures have been extracted (Tab.5), integrating the geometrical features with the soft-tissues landmarks and the plane *ndo* (plane joining *n* to *prn*) has been introduced in order to provide morphological information about the nose asymmetry (Fig.10).

Following the measuring strategies just explained and working over the five patients noses, the most significant data have been extracted on the first and third faces where the noses show positive shifts along *y* and *z* axes together with a reduction along *x* (Tab.6). Considering that the *n* (*nasion*) remains in the same location, before and after the surgery, and the conical frustum base has been subjected to a positive shift, this means that the nose has been subjected to a height reduction, as explained by CCA (Tab.3) with *N-SNA* (Fig.11).

	Description
$al_{right} - al_{left}$	nose width [*mm*].
n-prn-sn	nasal shift [*degree*]
n-prn	length of the nasal bridge [*mm*]
n-sn	nose height [*mm*]
plane ndo – n -prn	nasal asymmetry [*degree*].

Table 5: Nose morphological measures

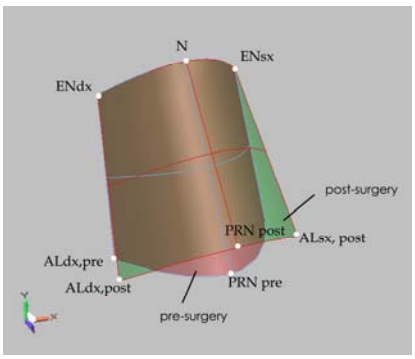

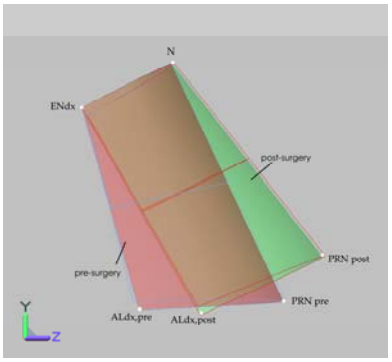

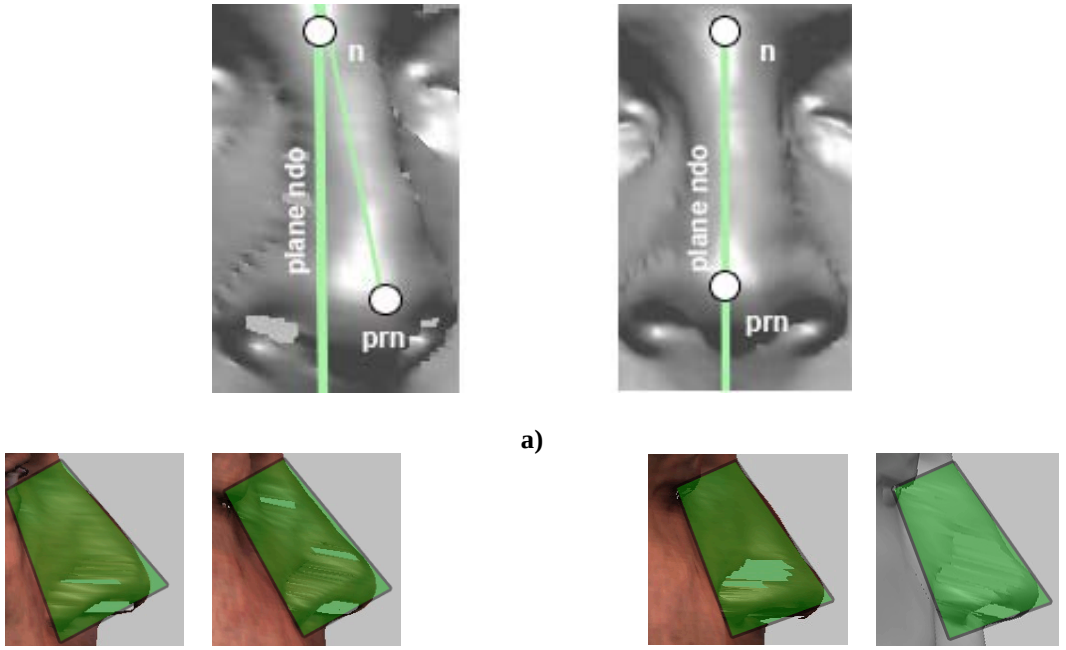

Figure 11: a) Geometrical Features comparison applied to the nose b) Class II & Class III

		Face 1		Face 2		Face 3		Face 4		Face 5	
		Pre	Post	Pre	Post	Pre	Post	Pre	Post	Pre	Post
Conical Frustum	al_{sx}-al_{dx} [mm]	*34.09*	*40.58*	*28.29*	*34.34*	*33.02*	*39.47*	*33.03*	*36.50*	*30.46*	*39.26*
	n $\hat{prn}$ sn [deg]	*99.98*	*110.02*	*91.10*	*94.93*	*86.22*	*92.21*	*108.92*	*100.46*	*94.69*	*98.22*
	n-prn [mm]	*44.12*	*45.11*	*45.62*	*46.19*	*45.41*	*48.43*	*43.14*	*46.41*	*43.90*	*45.95*
	n-sn [mm]	*49.25*	*53.30*	*51.30*	*51.79*	*51.96*	*51.88*	*51.11*	*51.67*	*49.38*	*52.09*
	plane ndo $\hat{n}$ prn [deg]	*1.18*	*0.50*	*1.13*	*0.54*	*1.03*	*1.40*	*3.81*	*2.25*	*1.90*	*1.03*

Table 6: Nose Measures applied to the Conical Frustum Feature

At the same as before for the nose some morphological measures have been extracted, integrating the geometrical features with the soft-tissues landmarks: *sn-gn* and *sn-plane b* for analysing *sn* and *gn* shifts, b_{sx}-b_{dx} , *b-gn* for analysing the facial width modifications and the shifts along *z*.

Following the measuring strategies just explained and working over the five patients noses, the most significant data have been extracted on the second and fifth faces where the mandible show positive shifts along *y* and *z* axes (Tab.7). Considering that the *b plane* remains in the same location, before and after the surgery, *sn* (subnasale) has been subjected to a positive shift along *y* and *gn* (gnathion) has been subjected to a positive shift both along *y* and *z*, this means that the ellipsoid feature has been subjected to an increasing. The same result has been provided by the CCA (Tab.3) with *SNA-ME* and (Tab.4) gnathion angle *ARGO – GOME* (Fig.12).

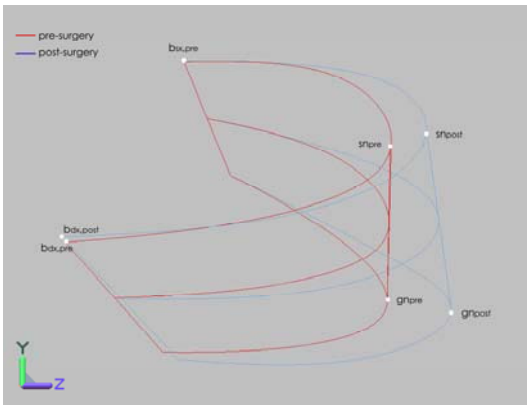

a)

b)

Figure 12: a) Geometrical Feature comparison method applied to the lower face portion b) Class II & Class III

		Face 1		Face 2		Face 3		Face 4		Face 5	
		Pre	**Post**	**Pre**	**Post**	**Pre**	**Post**	**Pre**	**Post**	**Pre**	**Post**
Ellipsoid	**sn-gn [mm]**	53.33	59.09	52.08	48.01	41.37	48.28	44	36.97	47.28	44.45
	sn-plane b [mm]	73.75	88.21	76.37	87.40	75.10	75.12	86.23	93.89	87.69	89.50
	b_{sx}-b_{dx} [mm]	154.91	150.99	149.46	152.76	139.32	135.45	131.34	133.54	134.14	133.78
	***b-gn*[mm]**	133.21	156.91	119.13	107.96	136.00	129.63	122.90	125.35	114.03	135.86

Table 7: Lower face portion measures applied to the Ellipsoid Feature

Case Studies: Geometrical Features Based vs Tetrahedral methodology Area Evaluation

In order to evaluate the performance of the proposed methodology in the area evaluation the geometrical features based approach has been compared with the tetrahedron one [1,2] (Tab.8) (Fig.13). Working on the five patients first of all the facial areas have been estimated employing the points cloud meshes and adding the area of every single triangles covering the different specific regions (Fig.14). The results coming from this evaluation has been considered as reference values, because the mesh approximation is very precise and depend only on the 3D scanner device employed for the acquisition. But using the mesh approximation it is possible to obtain only reliable information about the soft tissues area modifications, while it is impossible to understand, comparing pre and post surgery points cloud, where the face have been modified (shift, scaling, rotation, …). With the use of specific geometries, as those employed in the proposed method, on the contrary it is possible to extract simply spatial information, together with reliable data about area and volume.

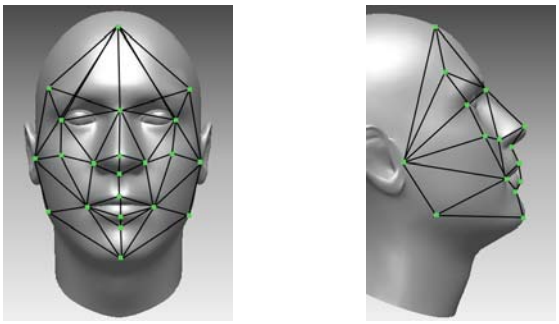

Figure 13: Area evaluation with the use tetrahedrons

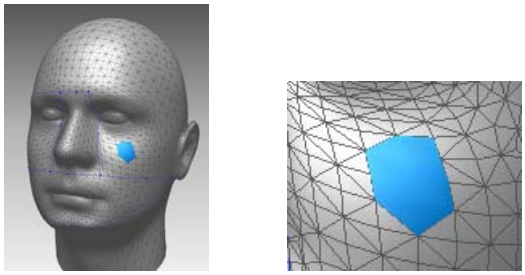

a) b)

Figure 14: Mesh area evaluation: a) an example of face points cloud meshed b) an example of selected triangles areas

[mm^2]	Face 1		Face 2		Face 3		Face 4		Face 5	
	Pre	**Post**	**Pre**	**Post**	**Pre**	**Post**	**Pre**	**Post**	**Pre**	**Post**
Conical Frustum	2183.26	2246.17	2324.85	2141.63	2359.21	2596.13	2343.86	2500.93	2663.50	2536.20
Nose Tetrahedron	1341.98	1618.31	1942.26	1669.64	2177.74	2273.94	1580.86	1820.12	1485.21	2085.59
Nose Meshes	3221.47	3771.69	3539.65	3591.95	3679.95	4365.19	4035.36	3978.58	4227.63	4187.56
Ellipsoid	10539.40	12669.58	8339.31	8896.12	8697.29	9456.12	9144.11	9510.31	8840.56	8728.69
Mandibole Tetrahedron	9175.87	9679.74	8861.11	8304.12	8761.83	8473.03	7268.64	8505.05	9102.36	9233.25
Mandibole Meshes	16345.25	15604.54	11178.46	11172.75	14299.50	13349.93	12471.27	13197.43	12048.99	14966.06

Table 8: Facial areas

As it is possible to see from the results coming from the different comparisons (Tab.9) the geometrical feature based approach show data more close to the real one then the tetrahedrons methodology.

[%]	Face 1		Face 2		Face 3		Face 4		Face 5	
	Pre	**Post**	**Pre**	**Post**	**Pre**	**Post**	**Pre**	**Post**	**Pre**	**Post**
Conical Frustum *vs* Nose Mesh	32	40	34	40	36	41	42	37	37	39
Nose Tetrahedron *vs* Nose Mesh	58	57	45	54	41	48	61	54	65	50
Ellipsoid *vs* Mandible Mesh	36	19	25	20	39	29	27	28	27	42
Mandibole Tetrahedron *vs* Mandible Mesh	44	38	21	26	39	37	42	36	24	38

Table 9: Differences between the evaluated area with the mesh methodology and those coming from the proposed methodology

Looking at the graphical comparison (Fig.15,16a) it is possible to see that the geometrical features based approach fits with good results the facial shape presenting only some anomalies, where the face profile is characterised by many curvature variations, as the labial zone. In this situation the tetrahedron approach shows better fitting results (Fig.15b).

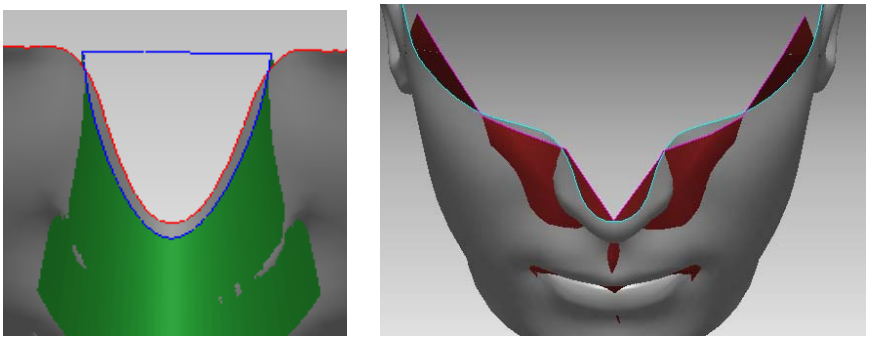

Figure 15: Featured based method applied to the nose a) Feature based method b) Tetrahedron Method

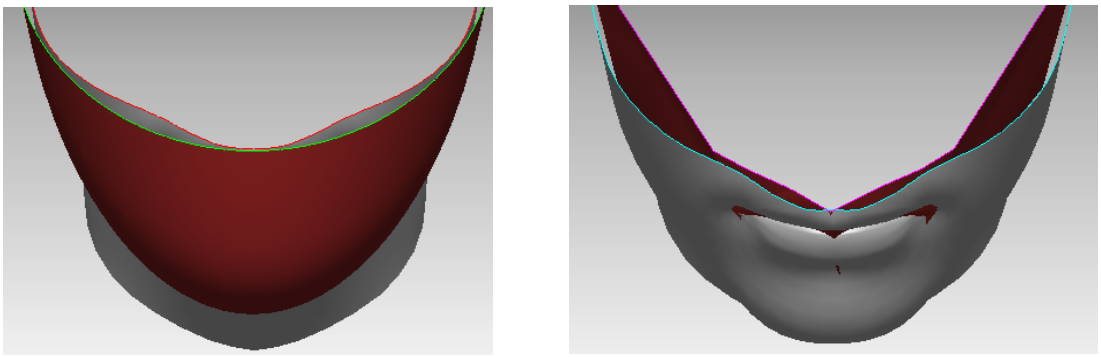

Figure 16: Featured based method applied to the mandible a) Feature based method b) Tetrahedron Method

On the contrary working on the nose profile while the geometrical feature based approach provides an efficient fitting behaviour (Fig.13a), the tetrahedron approach doesn't mach the real nose shape. This is justified by the fact that tetrahedral structure is composed of five vertices: *nasion, nose tip, left and right nose lobes, and nose base*. For instance looking at the nose top the while real shape shows one unique arc profile, connecting the eyebrows the tetrahedrons solution employ one point only.

This morphological mismatching between the real nose shape and the tetrahedron shape confirm the experimental data (Tab.7) that show a more reliable area evaluation working with the conical frustum instead of the tetrahedron.

Conclusions

As it is possible to see looking at the results obtained working with the case studies, the face decomposition with the use of solid geometries is able to provide a reliable information about the soft-tissue shift comparable with the traditional cephalometric data, but it is able also to provide a more complete set of three-dimensional information, as the facial area modification, that with the traditional methodology are not reachable. Comparing the area evaluation of the proposed methodology with the method that employs the tetrahedrons, it is possible to identify better results in those regions, where the tetrahedron method, due to the presence of flat faces it is obliged to cut the real facial profile. More than this the presence of elementary geometries that synthesises the real shape behaviour is able to support the use of 3D scanners for diagnostic purpose because provide few three-dimensional geometries, instead of huge points clouds that contain a big quantity of morphological data, but that are very difficult to employ and that sometimes, using the non appropriate measurements solutions, provide false information. Even the method has been proposed with the aim to study the quantification of post-operative changes, it could be a starting point also for other applications in medical diagnosis thanks to the possibility to synthesize many facial morphometric data using simple geometrical elements, more reliable than the simple tetrahedron.

References

[1] Ferrario V. F., Sforza C., Schmitz J. H., et al., Three-dimensional facial morphometric assessment of soft-tissue changes after orthognathic surgery, *Oral Surg Oral Med Oral Pathol Oral Radiol Endod*, 1999; **88**(5):549-556.

[2] Sforza C., Dellavia C., Tartaglia G. M., Ferrario V. F., Morphometry of the ear in Down's sindrome subjects. A three-dimensional computerized assessment, *Int J Oral Maxillofac Surg*, 2005; **34**:480-6.

[3] Chew M. T., Soft and hard tissue changes after bimaxillary surgery in Chinese class III patients, *Angle Orthod*, 2005; **75**:959-63.

[4] Koh C. H., Chew M. T., Predictability of soft tissue profile changes following bimaxillary surgery in skeletal class III Chinese patients, *J Oral Maxillofac Surg*, 2004; **62**:1505-1509.

[5] Hoffmann J., Westendorff C., Leitner C., et al., Validation of 3D-laser surface registration for image-guided cranio-maxillofacial surgery, *J Craniomaxillofac Surg*, 2005; **33**(1):13-18.

[6] Katsumata A., Fujishita M., Maeda M., et al., 3D-CT evaluation of facial asymmetry, *Oral Surg Oral Med Oral Pathol Oral Radiol Endod*, 2005; **99**(2):212-20.

[7] Mori A., Nakajima T., Kaneko T., et al., Analysis of 109 Japanese children's lip and nose shapes using 3-dimensional digitizer, *Br J Plast Surg*, 2005; **58**(3):318-329.

[8] Sforza C., Dellavia C., Colombo A., et al., Nasal dimensions in normal subjects. Conventional anthropometry versus computerized anthropometry, *Am J Med Genet*, 2004; **130A**:228-233.

[9] Hajeer M. Y., Ayoub A. F., Millett D. T., Three-dimensional assessment of facial soft-tissue asymmetry before and after orthognathic surgery, *Br J Oral Maxillofac Surg*, 2004; **42**:396-404.

[10] Soncul M., Bamber M. A. Evaluation of facial soft tissue changes with optical surface scan after surgical correction of Class III deformities, *J Oral Maxillofac Surg*, 2004; **62**(11):1331-1340.

[11] McIntyre G. T., Mossey P. A., Size and shape measurement in contemporary cephalometrics, *European Journal of Orthodontics* 2003; **25**:231-242.

[12] Harmon L. D., Khan M. K., Lashc R., Ramig P. F., Machine identification of human faces, *Pattern Recognition* 1981; **13**(2):97-110.

[13] Manual XLSTAT. http://www.xlstat.com/en/support/tutorials/gpa.htm [Accessibility verified April 21, 2008]

[14] Bookstein F. L., Morphometrics tools for landmark data, Cambridge: Cambridge University Press, 1991.

[15] Swiderski D. L., Morphological evolution of the scapula in three squirrels, chipmunks, and ground squirrels (Sciuridae): an analysis using thin-plate splines, *Evolution*, 1993; **47**:1854-1873.

[16] Richtsmeier J. T., Cheverud J.M., Lele S., Advances in anthropological morphometrics, *Ann Rev Anthropol*, 1992; **21**:283-305.

[17] Coombes A. M., Moss J. P., Linney A. D., Richards R, James DR. A mathematical method for comparison of three dimensional changes in the facial surface, *Eur J Orthod*, 1991; **13**:95-110.

[18] Raby G. P., Current principles of morphoanalysis and their implementations in oral surgical practice, *Br J Oral Surg*, 1977; **15**:97-109.

[19] Bush K., Antonyshyn O., Three-dimensional facial anthropometry using a laser surface scanner: validation of the technique, *Plast Reconstr Surg*, 1996; **98**(2):226-235.

[20] Hyun C. D., Dong Y. I., Uk L. S., Registration of multiple-range views using the reverse-calibration technique, *Pattern Recognition* 1998; **31**(4):457-464.

[21] Aung S. C., Ngim R. C., Lee S. T., Evaluation of the laser scanner as a surface measuring tool and its accuracy compared with direct facial anthropometric measurements, *Br J Plast Surg*. 1995; **48**:551-558.

[22] Tsang K. H. S., Cooke M. S., Comparison of cephalometric analysis using a non-radiographic sonic digitizer (DigiGraphTM Workstation) with conventional radiography, *European Journal of Orthodontics* 1999; **21**:1-13.

[23] Bhatia, S., S. Y. Bookheimer, I. D. Gaillard, W. Theodore: Measurement of whole temporal lobe and hippocampus for MR volumetry: normative data. Neurology 43 (1993) pp. 2006-2010

[24] Brann, B. S. IV, C. Wofsy, J. Wicks, J. Brayer: Quantification of neonatal cerebral ventricular volume by real-time Derivation and in vitro confirmation of a mathematical model. J. Ultrasound Med. 9 (1990) 1-8

[25] Cruz-Orive, L. M., N. Roberts: Unbiased volume estimation with coaxial sections: an application to the human bladder. J. Microsc. 170 (1993) 25-33

[26] Mayhew T. M., D. R. Olsen: Magnetic resonance imaging (MRI) and model-free estimates of brain volume determined using the Cavalieri principle. J. Anat. 178 (1991) 133-144

[27] Sforza C., Peretta R., Grandi G., Ferronato G., Ferrario V. F.: Soft tissue facial volumes and shape in skeletal Class III patients bifore and after orthognatic surgery treatment. JPRAS (2007) 60, 130-138

[28] Civardi Giovanni, La testa umana. Anatomia, Morfologia, Espressione per l'Artista, edizione Il Castello.

[29] Sergi G. 1895 On the Classification of Skulls, Science, Volume 1, Issue 24, pp. 658

[30] Beyer, W. H. CRC Standard Mathematical Tables, 28th ed. Boca Raton, FL: CRC Press, p. 227, 1987.

[31] Ferrario V. F., Sforza C., Serrao G., Ciusa V., Dellavia C., Growth and aging of facial soft-tissue: a computerised three-dimensional mesh diagram analysis, , 2003; **16**:420-33.

[32] Ferrario V. F., Sforza C., Ciusa V., Dellavia C., Tartaglia G. M., The effect of sex and age on facial asymmetry in healthy subjects: a cross-sectional study from adolescence to mid-adulthood,
J. Oral Maxillofac surg, 2001; **59**:382-388

[33] Yang X., Dong Y., Long X., Zhang G., Kao C., 2005, The evaluation of jaw function subsequent to bilateral sagittal split osteotomy, Oral Surgery, Oral Medicine, Oral Pathology, Oral Radiology, and Endodontology, Volume 100, Issue 1, July 2005, Pages 10-16